Jurnal Fisika 15 (1) (2025) 1-10
Jurnal Fisika
https://journal.unnes.ac.id/nju/index.php/jf/index

2D Numerical Modeling for Estimation of Run Up and Arrival Time of Tsunami at the Coast of Banyuwangi District

Alif Aulia Baroroh[1*], Supriyadi[1], Sutikno[1], Mochamad Aryono Adhi[1], Hamzah Latief[2]

[1]Department of Physics, Faculty of Mathematics and Natural Sciences, Universitas Negeri Semarang, Indonesia
[2]Department of Oceanography, Faculty of Earth Sciences and Technology, Institut Teknologi Bandung, Indonesia

Article Info

Article History:

Received:
10 January 2025

Accepted:
17 March 2025

Published:
5 May 2025

Keywords:
Tsunami, COMCOT, Banyuwangi

Abstract

The Banyuwangi tsunami was generated by an earthquake of magnitude 7.8 that struck the south coast of East Java with Mw 7.8 on June 3, 1994. The tsunami claimed the lives of more than 200 people, and severely damaged infrastructure, buildings and transportation facilities. Many studies have been conducted on the Banyuwangi tsunami, but not many have reviewed the validation of the maximum height compared to the results of field studies in the same year as the June 3, 1994 Banyuwangi tsunami. The study of Banyuwangi tsunami reconstruction aims to validate the maximum tsunami height of the model output compared to the results of field measurements by Tsuji in 1995. This study uses COMCOT v1.7 software with the nested model method. The results of the simulation of tsunami wave propagation that occurred every time period after the earthquake, showed that in snapshot layer 1 and layer 4 within 10 minutes the distribution of the earthquake expanded the tsunami wave propagation, within 30 minutes the tsunami wave propagation had entered several areas of the southern coast of East Java, within 35 minutes the tsunami wave propagation had reached land. The comparison ratio between model results and field measurements is K of 0.811998002 and κ (standard deviation) of 1.37536532 with an accuracy of 70% which shows a comparison of tsunami height simulation results are quite close to the tsunami height from field measurements.

✉ Correspondence address:
Department of Physics, Faculty of Mathematics and Natural Sciences,
Universitas Negeri Semarang, Indonesia
E-mail: alifauliab@students.unnes.ac.id

p-ISSN 2088-1509

INTRODUCTION

Tsunamis are one of the most devastating natural disasters that can occur in coastal areas (Röbke & Vött, 2017). They are caused by natural events such as earthquakes, volcanic eruptions or submarine landslides that cause large movements in the seabed and trigger powerful ocean waves (Kamigaichi, 2022). For example, tsunamis caused by earthquakes occurred in Sumatra and Andaman in 2004 and in Tohoku in 2011, tsunamis caused by volcanic eruptions occurred in Krakatoa in 1883, tsunamis caused by submarine landslides occurred in Papua New Guinea in 1998 (Farrell et al., 2015).

Seismicity is the main cause of tsunami occurrence. According to the tsunami catalog of the Geo Forschungs Zentrum Potsdam (GFZ-Postdam) in 2005, almost 82.3% of the 1,323 tsunamis recorded worldwide since the 17th century B.C., i.e. 1089 events, were caused by earthquakes (Schielein et al., 2007). During the period 1600 to 2007 approximately 184 tsunamis occurred in Indonesia. Of these, 90% were caused by tectonic earthquakes, 9% by volcanic eruptions and only 1% were triggered by landslides (Diposaptono & Budiman, 2006). The characteristics and conditions of an earthquake that can cause a tsunami are an earthquake magnitude of more than 6.5 on the Richter scale and an earthquake depth parameter of less than 100 km above sea level (Alfaris et al., 2020).

Indonesia is an archipelago located at the confluence of 3 tectonic plates (triple junction plate convergence), namely the Eurasian Plate, Pacific Ocean Plate and Indo- Australian Plate which collide with each other from time to time (Armono et al., 2021; Faiqoh et al., 2013). These plates are constantly moving (very slowly) and rubbing against each other along plate boundaries, known as faults. Plate boundaries cause an accumulation of energy as the plates lock together. When the lock between the plates is released, the accumulated energy is released in the form of earthquakes that can cause deformation of the seafloor. This deformation of the seabed can disrupt the water column above the earthquake area, causing a difference in sea level elevation which then travels as tsunami waves (Latief et al., 2011; Liu et al., 2009).

One of the tsunami-prone areas in Indonesia is the south coast of Java. On June 3, 1994 a 7.8 magnitude earthquake that caused a tsunami occurred on the south coast of East Java. The incident killed 250 people, injured 423 people, damaged 1,500 houses and sank or damaged 278 ships (Triyono et al., 2019). The earthquake that caused this tsunami is thought to have occurred at seismic gaps along the narrow seismic zone shown in Figure 1 (Setyonegoro, 2022).

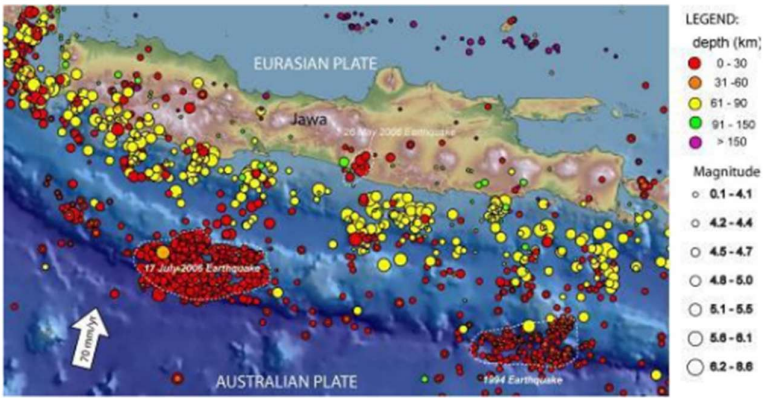

Figure 1. Modern seismicity in Java (Natawidjaja *et al.*, 2007).

Banyuwangi Regency is one of the southern coastal areas of East Java that was affected by the 1994 tsunami. Similar tsunami disasters may occur in the future, but the magnitude of the losses caused by tsunami disasters, especially casualties, damage to public facilities and other material losses, cannot be predicted, hence the need for tsunami disaster mitigation efforts. In order to reduce these losses, tsunami reconstruction and verification of model output with field survey results are required through tsunami wave propagation simulation modeling.

There have been many studies on the Banyuwangi tsunami, such as the reconstruction and modeling of tsunami propagation conducted by Febrianty et al., (2024) using the Toast system and conducted by Harahap (2019) using the Mike 21 flow model, but not many have examined the validation of the maximum tsunami height of the simulation results compared to the field measurement results in the same year as the June 3, 1994 Banyuwangi tsunami conducted by Tsuji et al., (1995). This study reconstructs the Banyuwangi tsunami to determine the run up value and arrival time of the tsunami by using COMCOT v1.7, a free software, which uses a multi-grid scheme that allows modeling with higher resolution in certain areas without having to increase the resolution in the entire domain, thus efficient in the use of computational resources and allowing faster and more detailed simulations in critical areas. With the reconstruction of past tsunamis, similar models can be applied in the prediction of tsunamis in the future at subduction areas to facilitate mitigation efforts.

METHOD

The method used in this research is 2D numerical modeling with a nested grid model. The equipment used is divided into two, namely hardware and software. The hardware used in this research, both for modeling and input data processing, was a computer system. The main softwares used in this study are shown in Table 1.

Table 1. Research softwares.

No	Tools	Function
1.	Software Global Mapper	Modeling and mapping input generation
2.	Software COMCOT v1.7	Modeling tsunami wave propagation
3.	Software MATLAB	Display the results of tsunami wave propagation modeling
4.	Software Ms.Excel	Plotting tide gauges and calculating earthquake parameters
5.	Software Notepad++	Editing text, data, and scripts of programming codes

The bathymetry data used to describe the topography of the seabed is BATNAS (National Bathymetry) data, while the topographic data used is DEMNAS (National Digital Elevation Model) data obtained from the website https://tanahair.indonesia.go.id/demnas/#. Earthquake parameters as input data for tsunami generation were obtained from Harvard Global Centroid Moment Tensor (Global CMT) research, shown in Table 2 below:

Table 2. Eartquake parameters.

Parameters	Size	Unit
Focal depth	15000	meters
Length of Fault Plane	127057	meters
Width of Fault Plane	38726	meters
Dislocation of Fault Plane	4.3	meters
Strike (θ)	278	degrees
Dip (δ)	7	degrees
Slip atau rake (λ)	89	degrees

To analyze tsunami reconstruction in detail, modeling using the nested grid model method is required. This nested grid method uses four different spatial grid designs, as shown in Figure 2.

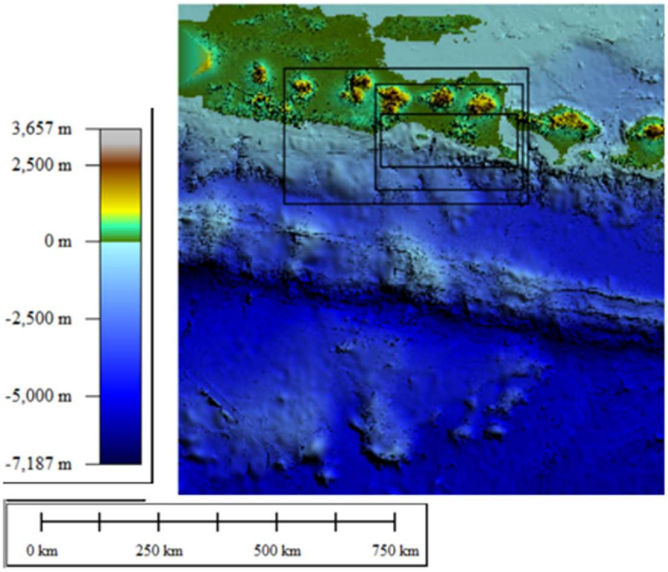

Figure 2. Domain nested grid.

To determine the validity of the modeling results, it is necessary to verify the simulation data with field data. The field measurement data used to verify the model are the results of field measurements made by Tsuji (1995) as shown in Figure 3. This data was obtained using traces of sea water inundation on the walls of houses and on the surface of tree bark in severely damaged villages, and also based on eyewitness reports from residents for beaches far from the tsunami source (Tsuji et al., 1995).

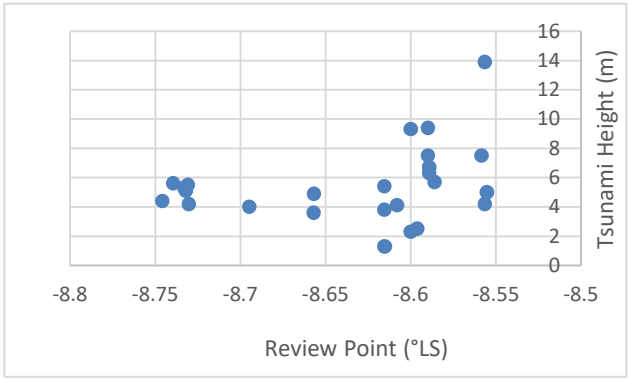

Figure 3. Tsunami height graph from field measurements made by Tsuji (1995).

To verify the simulation results, the simulated tsunami height is compared with the tsunami height from field observations. Aida (1978) introduced the parameter K which indicates the relative size of the height of the tsunami and simulation results, and K which indicates the precision of the simulated tsunami height (Gusman *et al.*, 2014). To evaluate the accuracy of the model, the geometric mean value of Aida (1978) K and its variance κ are used, which can be written as follows:

$$\log K = \frac{1}{n}\sum_{i=1}^{n} \log K_i \; ; \;\; K_i = \frac{O_i}{S_i} \tag{1}$$

$$\log \kappa = \left[\frac{1}{n}\sum_{i=1}^{n} (\log K_i)^2 - (\log K)^2\right]^{\frac{1}{2}} \tag{2}$$

where n is number of locations reviewed, O_i is the tsunami height from field observation at location- i, S_i is the numerically simulated tsunami height at location-i , and K_i is the ratio between observed and simulated tsunami height.

Shuto (in Muhari *et al.*, 2012) proposed value $0{,}8 < K < 1{,}2$ (20% error) and $\kappa < 1{,}45$ (variance tolerance) as criteria for confidence in the results simulation data. In addition, the Japan Society of Civil Engineers in (Takao, 2012) proposed a value of $0{,}95 < K < 1{,}05$ (5% error) and $\kappa < 1{,}45$ as confidence criteria for the simulation data results.

RESULTS AND DISCUSSION

The results obtained in this tsunami modeling include the initial condition of the water level in the sea around the epicenter at the time of the earthquake. The initial condition of a tsunami is a process of uplift and subsidence of the seabed caused by a shift in the earth's layers due to a sudden pull or pressure that causes the waves to rise out of the normal limits of sea water and cause a tsunami.

In the initial condition, the characteristics of tsunami wave arrival are shown by the initial decrease in wave height (low tide) at the coordinates of the tsunami source. The results of tsunami wave propagation modeling were processed using MATLAB software and the tsunami initial condition from the init plot is shown in Figure 4.

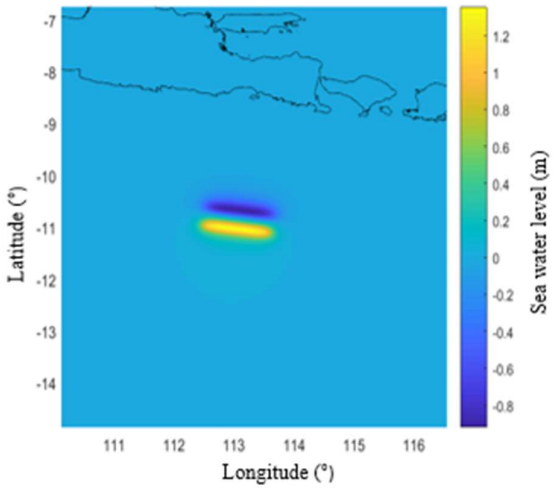

Figure 4. The initial condition of the tsunami.

Figure 4 shows that the sea water in the vicinity of an earthquake will rise 1.2m above sea level and fall 0.8m below sea level. The plot of zmax shows the maximum amplitude of the tsunami, as shown in Figure 5.

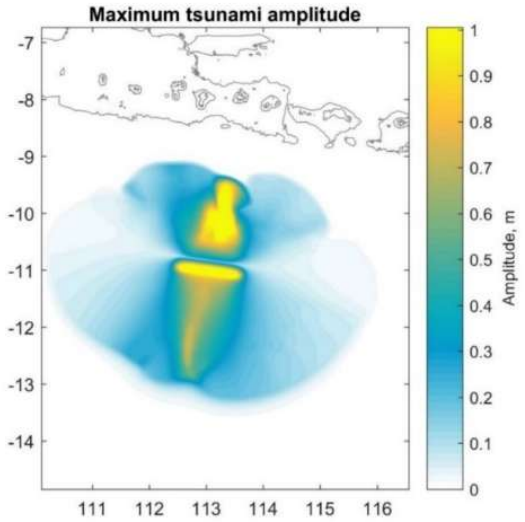

Figure 5. Maximum amplitude of the tsunami

The wave height (amplitude) of a tsunami is inversely proportional to the sea depth, so in coastal areas the amplitude is large. Tsunamis have a very high propagation speed, which can reach 200 m/s or 720 km/h on the high seas. When it reaches the coast, the tsunami wave speed decreases as the seawater silts up. Due to their long wavelengths, tsunamis have enormous energy. Theoretically, this is because the energy loss in wave propagation is inversely proportional to the wavelength. "Therefore, the closer to shore the tsunami wavelength is, the shorter it is, so it loses little energy in its propagation. Therefore, the destructive nature of tsunamis is due to their large amplitude and short wave length.

From the running results of COMCOT v1.7, tsunami wave propagation patterns were obtained and processed using MATLAB with snapshot plots. Several snapshots of tsunami wave propagation in layer 1 and layer 4 at different time periods can be seen in Figure 6 and Figure 7.

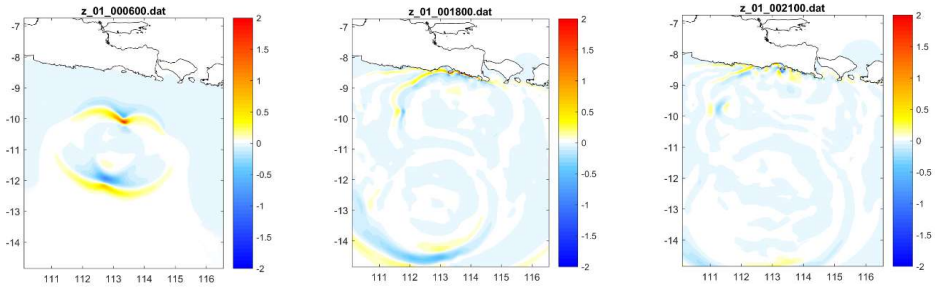

(a) (b) (c)

Figure 6. Snapshot of layer 1 at time (a) 10 minutes, (b) 30 minutes, and (c) 35 minutes

Figure 6 shows the results of the snapshot layer 1 at 10 minutes, where the earthquake extended the tsunami wave propagation. At 30 minutes, it can be seen that the tsunami waves had entered several areas of the southern coastline of East Java. At 35 minutes, it can be seen that the tsunami waves had already reached land.

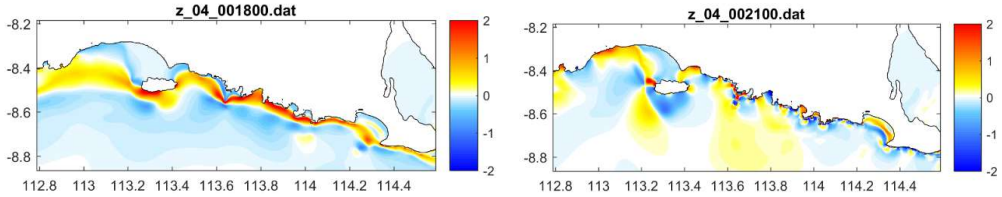

(a) (b)

Figure 7. Snapshot of layer 3 at time (a) 30 minutes and (b) 35 minutes.

In Figure 7, the results of the snapshot layer 4 at 30 minutes show that the tsunami waves have entered some areas of the southern coastline of Banyuwangi. At 35 minutes, it can be seen that the tsunami waves have reached the mainland. The blue colored seawater indicates that there is a decrease in sea level or tide, while the red and yellow colors indicate an increase in sea level.

From the model simulation with the nested grid system, the tsunami wave height at several virtual tide gauge points is obtained. The simulated tsunami heights will then be compared with the tsunami heights from field measurements made by Tsuji (1995) along the south coast of Banyuwangi. The tsunami heights at several points are shown in the graphs in Figure 8.

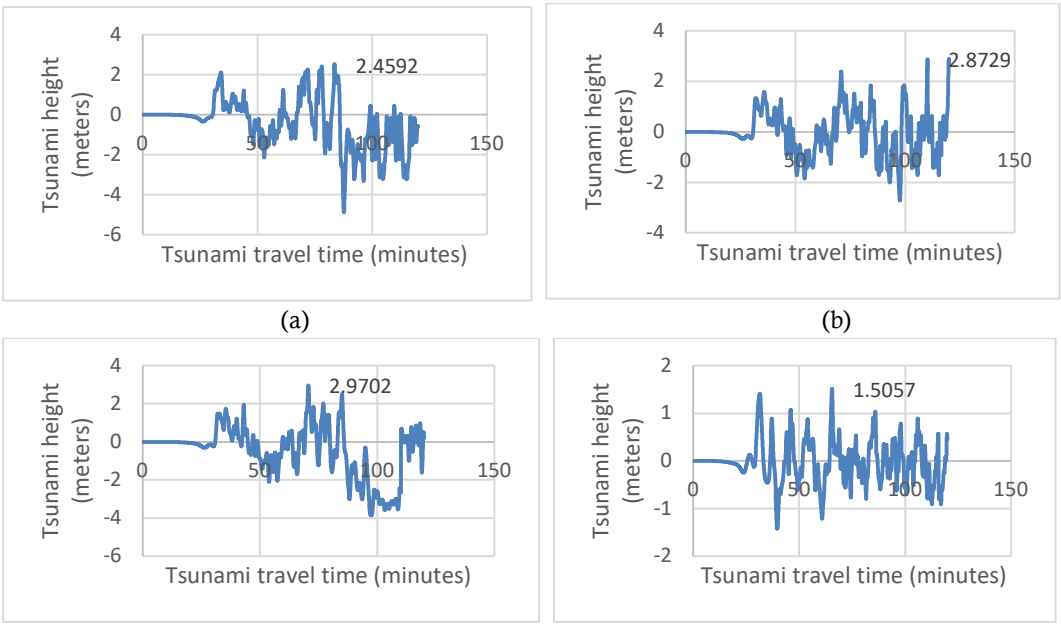

(a) (b)

(c) (d)

Figure 8. Graph of tsunami height at several points (a) Grajagan, (b) Grajagan Timur, (c) Purwoasri, (d) Lampon.

In Figure 8, the simulated tsunami height at several points is shown, namely (a) in the Grajagan area the tsunami height reached 2.45 meters, (b) in the East Grajagan area the tsunami height reached 2.87 meters, (c) in the Purwoasri area the tsunami height reached 2.9 meters, and (d) in the Lampon area the tsunami height reached 1.5 meters.

The simulated tsunami height is then compared with the field measurement results shown in Figure 9.

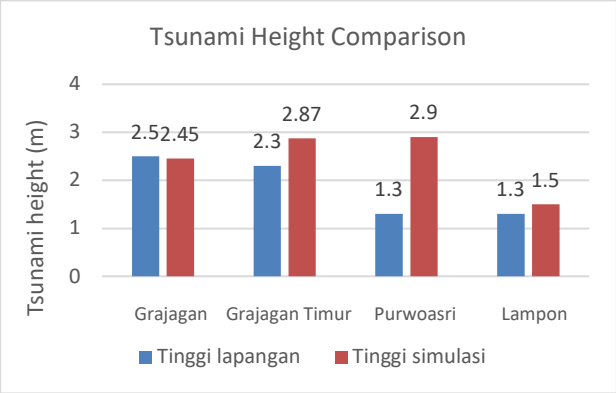

Figure 9. Comparison of simulated tsunami height with field measurements results.

In Figure 9, it can be seen that the difference between the simulated tsunami height and the field measurements in the Purwoasri area is quite large, because the topography of the sea around Purwoasri Beach tends to be sloping, allowing gradual changes in depth. This change is caused by natural processes that change the shape or condition of the environment little by little, such as erosion that slowly erodes the coastline. The comparison of simulated tsunami heights with field measurements shows that only a few points have a small difference and most points have a large difference, this is because the model simulation does not take into account the influence of friction and hydrostatic pressure on tsunami wave propagation and Manning's roughness. This is in accordance with the research conducted by Setyonegoro (2022) using 3 different model parameters, namely model 1 and model 2 that do not take into account, while model 3 with the Manning's roughness coefficient does it takes into account the influence of friction force, hydrostatic pressure on tsunami wave propagation and Manning's roughness. The results of model 1 and model 2 show that the tsunami run-up difference between the model and the run-up of the field survey results is very large, namely >12 m. Meanwhile, model 3 has a tsunami run-up difference between the model and the run-up of the field survey results of only 0.33%. Meanwhile, model 3 has a tsunami run-up difference between the model and the run-up of the field survey results of only 0.33 m.

To verify the simulation results, the simulated tsunami height was compared with the tsunami height from field measurements using the Aida verification method. Shuto in Muhari et al. (2012) proposed values of $0{,}8 < K < 1{,}2$ (20% error) and $\kappa < 1{,}45$ (variance tolerance) as confidence criteria for the simulation data results. The simulation results produce a K value of 0.811998002 and κ which indicates the precision of the simulated tsunami height of 1.37536532 with an accuracy of 70% which shows the comparison of tsunami height simulation results are already close to the tsunami height from field observations

CONCLUSION

From the results of running COMCOT v1.7, a simulation of the tsunami wave propagation that occurred at each time period after the earthquake, can be seen from the results of snapshot layer 1 and layer 4 at 10 minutes the distribution of the earthquake expanded the tsunami wave propagation, at 30 minutes the tsunami wave propagation was seen to have entered several areas of the southern coast of East Java, at 35 minutes the tsunami wave propagation was seen to have reached land. By using Aida verification, the simulated tsunami height is compared with the tsunami height observed in the field and the value is obtained K 0.811998002 and κ 1.37536532 with an accuracy of 70% which shows that the comparison of the simulated tsunami height is quite close to the simulated tsunami height field observation.

ACKNOWLEDGEMENT

The authors would like to thank Universitas Negeri Semarang for providing research funding facilities through grant number: DPA 023.17.2.690645/2024.10.

REFERENCE

Aida. (1978). Reliability of a Tsunami Source Model Derived from Fault Parameters. *J. Phys. Earth*, *26*, 57–73.

Alfaris, L., Baswantara, A., & Suhernalis. (2020). Numerical Analysis Of Pangandaran Tsunami. *Marine and Fisheries Science Technology Journal*, *1*(1), 39–45.

Armono, H. D., Putra, A. R., & Wahyudi. (2021). Analysis of Tsunami Wave Height, Run-up, and Inundation in the Coastal of Blitar and Malang Regency. *IOP Conference Series: Earth and Environmental Science*, *936*(1). https://doi.org/10.1088/1755-1315/936/1/012013.

Diposaptono S., dan Budiman. 2006. Tsunami. Buku Ilmiah Populer, Jakarta.

Faiqoh, I., Gaol, J. L., & Ling, M. M. (2013). Vulnerability level map of tsunami disaster in Pangandaran Beach, West Java. International Journal of Remote Sensing and Earth Sciences (IJReSES), 10(2).

Farrell, E. J., Ellis, J. T., & Hickey, K. R. (2015). Tsunami Case Studies. In *Coastal and Marine Hazards, Risks, and Disasters* (Issue February). https://doi.org/10.1016/B978-0-12-396483-0.00004-2

Febrianty, A., Ramadhanty, A. Z., Nurokhim, A., & Widodo, A. (2024). Rekonstruksi dan Pemodelan Penjalaran Tsunami menggunakan Sistem Toast dengan Metode Pemodelan Easywave (Studi Kasus Tsunami Banyuwangi 3 Juni 1994). *Jurnal Pendidikan Geografi Undiksha*, *12*(2), 181–190. https://ejournal.undiksha.ac.id/index.php/JJPG

Gusman, A. R., Tanioka, Y., Macinnes, B. T., & Tsushima, H. (2014). A methodology for near-field tsunami inundation forecasting: Application to the 2011 Tohoku tsunami. *AGU: Journal of Geophysical Research, Solid Earth*, *119*. https://doi.org/10.1002/2014JB010958.

Harahap, R. G. (2019). Rekonstruksi dan Simulasi Penjalaran Tsunami Banyuwangi 1994 Menggunakan Mike 21 Flow Model. *Inovtek Polbeng*, *9*(1), 66. https://doi.org/10.35314/ip.v9i1.900.

Kamigaichi, O (2022). Tsunami forecasting and warning. *Complexity in tsunamis, volcanoes, and their hazards*, Springer. https://doi.org/10.1007/978-1-0716-1705-2_568.

Latief, H., D.O. Ismoyo, I.R. Pranantyo, R.G. Munthe, 2011, Pemodelan Tsunami Kepulauan Mentawai, Fakultas Ilmu dan Teknologi Kebumian, Institut Teknologi Bandung, Bandung.

Liu, P. L. F., Wang, X., & Salisbury, A. J. (2009). Tsunami Hazard and Forecast Study in South China Sea. *Journal of Asian Earth Sciences*, *36*(1), 2–12.

Muhari, A., Imamura, F., Supassri, A., & Mas, E. (2012). Tsunami Arrival Time Characteristics of the 2011 East Japan Tsunami Obtained from Eyewitness Accounts, Evidence and Numerical Simulation. *Journal of Natural Disaster Science*, *34*(1), 91–104.

Natawidjaja, D. H., Sieh, K., Galetzka, J., Suwargadi, B. W., Cheng, H., Edwards, R. L., & Chlieh, M. (2007). Interseismic deformation above the Sunda Megathrust recorded in coral microatolls of the Mentawai islands, West Sumatra. *Journal of Geophysical Research: Solid Earth*, *112*(2), 1–27. https://doi.org/10.1029/2006JB004450

Röbke, B. R., & Vött, A. (2017). The tsunami phenomenon. *Progress in Oceanography*, *159*(September), 296–322. https://doi.org/10.1016/j.pocean.2017.09.003

Schielein, P., Zschau, J., Woith, H., Schellmann, G., 2007. Tsunamigefährdung im Mittelmeer—Eine Analyse geomorphologischer und historischer Zeugnisse. In: Schellmann, G. (Ed.), Bamberger Geographische Schriften, vol. 22, pp. 153–199.

Setyonegoro, W. (2022). Pengaruh Gaya Gesek Dan Tekanan Hidrostatik Pada Propagasi Tsunami (Studi Kasus: Tsunami Jawa Timur 3 Juni 1994). *Buletin Meteorologi, Klimatologi, Dan Geofisika*,

3(3), 18–41.

Shuto, N., 1991, Numerical Simulation of Tsunami – Its Present and Near Future, Natural Hazards, 4(2-3), 171–191.

Triyono, R, Prasetya, T, Daryono, ASD, Sudrajat, A. (2019). Katalog Tsunami Indonesia Tahun 416-2018. *Jakarta: BMKG*.

Tsuji, Y., Imamura, F., Matsutomi, H., Synolakis, C. E., Nanang, P. T., Jumadi, Harada, S., Han, S. S., Arai, K., & Cook, B. (1995). Field survey of the East Java earthquake and tsunami of June 3, 1994. *Pure and Applied Geophysics PAGEOPH*, *144*(3–4), 839–854. https://doi.org/10.1007/BF00874397.

Wang, X., 2009, User Manual for Comcot Version 1.7, Cornell University, USA.

Wells, D., dan Coppersmith, K., 1994, New Empirical Relationships among Magnitude, Rupture Length, Rupture Width, Rupture Area, and Surface Displacement, Bulletin of the Seismological Society of America, 4, 84, 974-1002.